

1 **A novel intrinsically disordered outer membrane lipoprotein of**
2 ***Aggregatibacter actinomycetemcomitans* binds various cytokines and plays a**
3 **role in biofilm response to interleukin-1 β and interleukin-8**

4 Tuuli Ahlstrand^a, Heidi Tuominen^a, Arzu Beklen^a, Annamari Torittu^a, Jan Oscarsson^b, Raija
5 Sormunen^c, Marja T. Pöllänen^d, Perttu Permi^{e,f,g}, Riikka Ihalin^a

6 a) Department of Biochemistry, University of Turku, Turku, Finland

7 b) Oral Microbiology, Department of Odontology, Umeå University, Umeå, Sweden

8 c) Biocenter Oulu and Department of Pathology, University of Oulu, Oulu Finland

9 d) Institute of Dentistry, University of Turku, Turku, Finland

10 e) Program in Structural Biology and Biophysics, Institute of Biotechnology, University of
11 Helsinki, Helsinki, Finland

12 f) Department of Biological and Environmental Sciences, Nanoscience Center, University of
13 Jyväskylä, Jyväskylä, Finland

14 g) Department of Chemistry, Nanoscience Center, University of Jyväskylä, Jyväskylä, Finland

15 Keywords: intrinsically disordered protein, bacterial cytokine receptor, outer membrane lipoprotein,
16 *Aggregatibacter actinomycetemcomitans*; biofilm matrix composition

17

18 Abbreviations and acronyms: BilRI, bacterial interleukin receptor I; BSA, bovine serum albumin;
19 CFUs, colony forming units; ClfA, clumping factor A; DsrA, Ducreyi serum resistance A; eDNA,
20 extracellular DNA; ELISA, enzyme-linked immunosorbent assay; FgbA, fibrinogen binder A; FID,
21 free induction decay; HGF, human gingival fibroblast; HGK, human gingival keratinocyte; HSQC,
22 heteronuclear single quantum coherence spectroscopy; IDP, intrinsically disordered protein; IL,
23 interleukin; IFN, interferon; IPTG, isopropyl β -D-1-thiogalactopyranoside; *ltxP*, leucotoxin promoter;
24 MALDI TOF MS, matrix-assisted laser desorption/ionization time-of-flight mass spectrometry; NMR,
25 nuclear magnetic resonance; OPG, osteoprotegerin; PAMP, pathogen-associated molecular pattern;
26 PGA, poly-N-acetylglucosamine; PMSF, phenylmethylsulfonyl fluoride; RANK, receptor activator of
27 nuclear factor κ -B; RANKL, RANK ligand; RT, room temperature; sIL-6R, soluble IL-6 receptor;
28 TGF, transforming growth factor; TNF, tumour necrosis factor; TSA, tryptone soy agar; TSB,
29 tryptone soy broth

30

31 **ABSTRACT**

32 Intrinsically disordered proteins (IDPs) do not have a well-defined and stable three-dimensional fold.
33 Some IDPs can function as either transient or permanent binders of other proteins and may interact
34 with an array of ligands by adopting different conformations. A novel outer membrane lipoprotein,
35 bacterial interleukin receptor I (BilRI) of the opportunistic oral pathogen *Aggregatibacter*
36 *actinomycetemcomitans* binds a key gatekeeper proinflammatory cytokine interleukin (IL)-1 β .
37 Because the amino acid sequence of the novel lipoprotein resembles that of fibrinogen binder A of
38 *Haemophilus ducreyi*, BilRI could have the potential to bind other proteins, such as host matrix
39 proteins. However, from the tested host matrix proteins, BilRI interacted with neither collagen nor
40 fibrinogen. Instead, the recombinant non-lipidated BilRI, which was intrinsically disordered, bound
41 various pro/anti-inflammatory cytokines, such as IL-8, tumour necrosis factor (TNF)- α , interferon
42 (IFN)- γ and IL-10. Moreover, BilRI played a role in the *in vitro* sensing of IL-1 β and IL-8 because
43 low concentrations of cytokines did not decrease the amount of extracellular DNA in the matrix of
44 *bilRI* mutant biofilm as they did in the matrix of wild-type biofilm when the biofilms were exposed to
45 recombinant cytokines for 22 hours. BilRI played a role in the internalization of IL-1 β in the gingival
46 model system but did not affect either IL-8 or IL-6 uptake. However, *bilRI* deletion did not entirely
47 prevent IL-1 β internalization, and the binding of cytokines to BilRI was relatively weak. Thus, BilRI
48 might sequester cytokines on the surface of *A. actinomycetemcomitans* to facilitate the internalization
49 process in low local cytokine concentrations.

50 Introduction

51 Intrinsically disordered proteins (IDPs) go against the *structure-defines-function* paradigm given that
52 they lack a well-defined three-dimensional fold; yet, they are elementary components in a myriad of
53 cellular processes.¹ The proportion of IDP increases when moving from simple microorganisms to
54 more complex eukaryotes, suggesting an evolutionary advantage of having flexible proteins that may
55 possess several functions. For instance, the proteome of *Escherichia coli* has been predicted to contain
56 approximately 15% proteins having more than 30 amino acid disordered segments, whereas in
57 *Saccharomyces cerevisiae*, the ratio is approximately 50-60%.² In eukaryotes, many IDPs have roles
58 in signal transduction, where they may bind to multiple ligands with variable affinities.³

59 The oral opportunistic pathogen *Aggregatibacter actinomycetemcomitans* can be found from
60 multispecies biofilms in diseased periodontal pockets of patients suffering from aggressive or chronic
61 forms of periodontitis.⁴⁻⁶ Among the diverse changes in the host response to multispecies biofilms,
62 periodontal diseases are characterized by alterations in the levels of various inflammatory cytokines,
63 such as interleukin (IL)-1 β , IL-6, and IL-8, and the anti-inflammatory cytokine IL-10.⁷ The highly
64 leucotoxic JP2 genotype of *A. actinomycetemcomitans* has been suggested to be an important
65 aetiological agent in disease initiation,⁸ where the inflammatory reaction is caused by inflammophilic
66 dysbiotic multispecies bacterial biofilm whose existence may be favoured by the micromilieu in
67 inflammation.⁹ This biofilm grows attached to the tooth surface and invades between the tooth and
68 gingival tissue towards the junctional epithelium.¹⁰ The host tissue, including alveolar bone, is mainly
69 destroyed by the host response to the pathogenic biofilm. *A. actinomycetemcomitans* may have
70 systemic effects on host health because it has been linked to the aetiology of cardiovascular
71 diseases,^{11,12} endocarditis,¹³ and brain abscesses.¹⁴ Thus, its pathogenic properties may have broader
72 significance to human health than merely oral health.

73 Human pathogens have several strategies to disturb and evade the host innate immune defence
74 systems. Bacterial cells may grow as protective communities known as biofilms, in which the
75 extracellular matrix provides protection from antibodies, antibiotics and cellular immune defence
76 cells, such as macrophages.¹⁵ Adhesive type IV Fli-pili, poly-N-acetylglucosamine (PGA) and

77 extracellular DNA (eDNA) are the main biofilm matrix components of *A. actinomycetemcomitans*.¹⁶
78 ¹⁷ Of these, long bundled Flp-pili protein fibre plays the most important role in autoaggregation,
79 nonspecific adherence, biofilm formation and virulence in a rat model.¹⁷⁻²⁰
80 Various pathogens possess receptors that bind host inflammatory cytokines.²¹⁻²⁴ The binding of
81 cytokines to bacteria may change the properties of the bacteria, such as their biofilm formation^{25, 26}
82 and virulence gene expression,^{21, 23, 27} and may also manipulate complex host inflammatory reactions,
83 leading to debilitated host defence against colonizing or invading pathogens. We have shown that *A.*
84 *actinomycetemcomitans* is able to bind the central proinflammatory cytokine IL-1 β ²⁶ and to
85 internalize IL-1 β ^{26, 28} and that intracellular IL-1 β binds to at least two bacterial proteins^{26, 28}. In
86 addition, IL-1 β decreases the metabolic activity of *A. actinomycetemcomitans* biofilms.²⁶ In our recent
87 study, we have identified an outer membrane lipoprotein of *A. actinomycetemcomitans*, bacterial
88 interleukin receptor I (BilRI),²⁴ which is most likely one of the first-line binders of IL-1 β on the
89 extracellular side of the bacterium. Whether this novel outer membrane protein is involved merely in
90 the response of *A. actinomycetemcomitans* biofilm to IL-1 β or whether it could bind host proteins and
91 cytokines other than IL-1 β was not known. Thus, the aims of the present study was to resolve the
92 three-dimensional structure of BilRI, to investigate the host protein- and cytokine-binding capacity of
93 the *Pasteurellaceae*-specific BilRI and to study the phenotype and response to cytokines of a single-
94 gene-deletion mutant of *bilRI*.
95 Our results indicate that BilRI is not a specific receptor of IL-1 β *in vitro* and binds to other
96 inflammatory cytokines, such as IL-8 and IL-10. We also found that BilRI is an IDP, which most
97 likely explains the existence of several ligands. *bilRI* deletion did not completely prevent cytokine
98 internalization, but it significantly decreased IL-1 β uptake and impeded the response of biofilm to low
99 concentrations of IL-1 β and IL-8. Because the binding of cytokines to the BilRI was relatively weak,
100 BilRI might function as a non-specific cytokine concentrator on the surface of *A.*
101 *actinomycetemcomitans* that facilitates the internalization process, especially in low concentrations of
102 cytokines.

103 Results

104 *BilRI is an intrinsically disordered protein*

105 The proton (^1H) spectrum of BilRI measured at 600 MHz exhibits features typical of a disordered
106 protein, including a collapsed chemical shift dispersion in the amide proton region (8.2 ± 0.3 ^1H ppm)
107 and the lack of shielded methyl protons, i.e., clustering of methyl protons to so-called random coil
108 shift, 0.7 ppm (Fig. 1A). To confirm these observations, we also performed a two-dimensional ^1H ,
109 ^{15}N heteronuclear single-quantum coherence (^{15}N HSQC) experiment at the 800-MHz ^1H frequency
110 of BilRI (Fig. 1B). To slow down the chemical exchange of labile amide protons with solvent protons,
111 we measured the ^{15}N HSQC spectrum of BilRI under mildly acidic conditions (pH 5). This spectrum
112 more clearly highlights the same features already visible in the corresponding ^1H spectrum, i.e., poor
113 dispersion of amide proton chemical shifts, indicating that BilRI remains disordered in solution and
114 under slightly acidic conditions.²⁹ The amino acid sequence analysis supported this finding, showing
115 high numbers of charged and polar residues and a low number of hydrophobic bulky amino acids
116 (Fig. 1C). Moreover, the BilRI sequence had a low complexity, i.e., biased amino acid composition: it
117 did not have any aromatic amino acids, such as phenylalanine, tyrosine and tryptophan, and 48% of
118 the sequence is made up of three residues: alanine, lysine and aspartate (Fig. 1C). All of the above-
119 mentioned amino acid sequence features are typical for IDPs.

120 *Recombinant BilRI binds to various cytokines but not to the host matrix proteins collagen* 121 *and fibrinogen*

122 A microplate assay showed that recombinant BilRI bound to various cytokines, of which the binding
123 to IL-8 was high compared with the binding of BilRI to the negative control protein bovine serum
124 albumin (BSA; $p=0.008$; paired-samples T-test; Fig. 2A). However, the binding to IL-6-coated wells
125 was weak and almost as inefficient as the binding to BSA, which was used as a blocking agent in the
126 assay (Fig. 2A). We decided to use C-tagged recombinant BilRI in our binding assays because
127 binding to IL-1 β was originally shown with a similar protein.²⁴ However, we also tested an N-tagged
128 variant of BilRI, which did not show increased binding to IL-1 β , IL-8, or IL-6 compared with the C-

129 tagged protein (data not shown). BilRI did not bind to fibrinogen- (Fig. 2B) or to collagen (Fig. 2C)-
130 coated wells. Moreover, BilRI binding to IL-8 was weaker than the fibrinogen-binding of positive
131 control protein clumping factor A (ClfA) of *S. aureus* and the collagen-binding of positive control
132 protein YadA of *Yersinia enterocolitica* (Fig. 2C).

133 ***Viable biofilm of wild-type A. actinomycetemcomitans bound IL-8 and IL-6***

134 When wild-type *A. actinomycetemcomitans* biofilm was co-cultured together with an organotypic
135 gingival mucosa in the absence of antibiotics, the biofilm sequestered both IL-8 and IL-6 (Fig. 3A).
136 However, when the co-culture was performed in the presence of antibiotics, which decreased the
137 viability of the biofilm,²⁸ the immunohistological staining of the biofilm with anti-IL-8 and anti-IL-6
138 was faint (Fig. 3A). However, the epithelium contained more cytokines in the presence than in the
139 absence of antibiotics (Fig. 3A). In addition, the growth medium contained slightly elevated amounts
140 of IL-6 and IL-8 (Fig. 3B) when antibiotics were used in the biofilm-gingival tissue co-culture,
141 suggesting that the cytokines leaked from the system when not sequestered by the viable biofilm.
142 However, due to inter-sample variance, the difference was not statistically significant. In similar
143 organotypic gingival tissue – biofilm co-cultures with a slightly thinner keratinocyte layer²⁸ *A.*
144 *actinomycetemcomitans* cells efficiently internalized IL-1 β (Fig. 3C).

145 ***Deletion of stand-alone gene bilRI altered the biofilm matrix composition in rich medium***

146 The prokaryotic operon database (ProOpDB, <http://operons.ibt.unam.mx/OperonPredictor>)³⁰
147 predicted that *bilRI* is a stand-alone gene. When cultured on blood agar plates, the single-gene-
148 deletion mutant of *bilRI* produced typical colonies with a rough colony morphology (Fig. 4A).
149 Although the *bilRI* mutant colonies were slightly more adherent to the agar than the wild-type
150 colonies, cell suspensions³¹ could be produced similarly from both strains (Fig. 4B). However, BilRI
151 overexpression resulted in a tiny colony size, and only small amounts of bacteria could be harvested
152 from the plates. Nonetheless, an even cell suspension could be attained (Fig. 4B). The *bilRI* mutant
153 formed as much biofilm as the wild-type strain in rich medium, whereas the overexpression of BilRI
154 in *A. actinomycetemcomitans* almost completely disappeared the cell's capacity to form biofilm
155 ($p=0.0003$, paired-samples T-test with Bonferroni corrections) (Fig. 4C). In biofilm, the cell

156 morphology of *bilRI* mutants did not differ from the morphology of the wild-type strain (Fig. 4D).
157 BilRI overexpression appeared to cause outer membrane lysis (Fig. 4D), explaining the tiny colonies
158 (Fig. 4A) and small cell size (Fig. 4D). In rich medium, the young biofilm, *i.e.*, the biofilm that had
159 not started to detach by releasing cells into the medium,³² of the *bilRI* mutant strain contained more
160 total protein in proportion to the biofilm mass than the wild-type *A. actinomycetemcomitans* strain
161 ($p=0.009$; Mann-Whitney U-test) (Fig. 5A). In contrast, the *bilRI* mutant biofilm contained less
162 eDNA than the wild-type strain ($p=0.021$; Mann-Whitney U-test) (Fig. 5B). Because some outer
163 membrane proteins of *A. actinomycetemcomitans* or close relative species bind to host proteins, such
164 as collagen and fibrinogen, we studied the binding of the *bilRI* mutant to these host proteins. *bilRI*
165 deletion did not decrease the binding of *A. actinomycetemcomitans* to either fibrinogen- or collagen-
166 coated wells (Fig. 5C). In contrast, the *bilRI* mutant bound collagen slightly more efficiently than the
167 corresponding wild-type strain, but the difference was not statistically significant ($p=0.275$; Mann-
168 Whitney U-test, Fig. 5C).

169 ***BilRI played a role in IL-1 β internalization***

170 Because the viable biofilm of wild-type *A. actinomycetemcomitans* bound both IL-8 and IL-6, the
171 uptake of these cytokines and the role of BilRI in their uptake were studied by incubating *A.*
172 *actinomycetemcomitans* wild-type and *bilRI* biofilms with gingival keratinocyte monolayers.
173 Previously reported IL-1 β uptake²⁸ was used as a positive control. The wild-type *A.*
174 *actinomycetemcomitans* biofilm cells internalized IL-8, IL-6, and IL-1 β (Fig. 6A) in these conditions.
175 When *bilRI* was deleted from the *A. actinomycetemcomitans* genome, the amount of IL-1 β inside and
176 attached to the biofilm cells, which were co-cultured with human gingival epithelial cells, was
177 significantly lower than for corresponding wild-type cells ($p=0.007$; Mann-Whitney U-test, Figs. 6A
178 and 6B). However, the *bilRI* mutant cells did not differ from the wild-type cells in their IL-8 and IL-6
179 uptake efficiencies ($p=0.649$ and $p=0.128$, respectively; Mann-Whitney U-test, Fig. 6A and B).

180 ***Deletion of bilRI abolished biofilm response to IL-1 β and IL-8***

181 When exposed to low concentrations of IL-1 β and IL-8, the matrix composition of the wild-type
182 biofilm changed, *i.e.*, the amount of eDNA decreased, whereas the amount of PGA, total protein and

183 total biofilm mass remained unchanged (Table 2). The deletion of *bilRI* rendered the biofilm
184 unresponsive to IL-1 β and IL-8, as determined by measuring the composition of the biofilm (Table 2).

185 Discussion

186 Although IL-1 β was the cytokine that was originally used in the identification of BilRI, it was only
187 moderately bound by this bacterial protein compared with the other tested cytokines. Our novel
188 finding that BilRI is an IDP could explain the existence of multiple ligands. The results of the nuclear
189 magnetic resonance (NMR) studies, which indicated the absence of a specific fold, were supported by
190 the amino acid analysis showing high numbers of charged and polar residues and a low number of
191 hydrophobic bulky amino acids, a composition that is typical for IDPs.¹ In addition, the BilRI
192 sequence had low complexity: it lacks all aromatic amino acids, such as phenylalanine, tyrosine and
193 tryptophan, and 48% of the sequence is made up of three residues: alanine, lysine and aspartate. The
194 unadorned peptides of IDPs are often involved in molecular interactions, in which they may bind the
195 ligand with variable affinities. Thus, an IDP can function as a scavenger/effector protein if it has a
196 strong affinity or as a chaperone/recognition motif if it has a weak affinity for its ligands.³³ Our results
197 confirmed that BilRI had relatively weak affinity for the cytokines, suggesting that it might function
198 as a cytokine concentrator in the outer membrane of *A. actinomycetemcomitans* binding cytokines
199 only temporarily before sending them forward to the next binding motif in the internalization chain.
200 This hypothesis was supported by the observation that the deletion of *bilRI* did not completely inhibit
201 the internalization of IL-1 β but significantly decreased the uptake efficacy.
202 Various molecules released by the *A. actinomycetemcomitans* biofilm are known to induce IL-8 and
203 IL-6 production in human whole blood.³⁴ Because IL-8 showed the highest affinity to BilRI, it was
204 selected for further studies to investigate whether it affects the composition of *A.*
205 *actinomycetemcomitans* biofilm and is internalized by the biofilm cells in a BilRI-dependent or BilRI-
206 independent manner. *A. actinomycetemcomitans* responded to BilRI in a manner dependent on low
207 concentrations (10 ng/ml) of IL-1 β and IL-8 by decreasing the eDNA amount in biofilm. This was the
208 only observed change in the biofilm composition because the cytokines did not alter either the PGA or
209 total protein amounts. Moreover, the total biofilm mass did not change in response to the cytokines. In
210 general, eDNA is suggested to play an important role in the early stages of biofilm development,
211 enhancing adhesion to the surface and stabilizing the young biofilm (for a review, see ref. ³⁵).

212 Although eDNA protects at least young biofilms from antimicrobial agents,³⁶ host defence factors,³⁷
213 and mechanical stress,³⁸ it may also compromise the bacterial viability by acting as a pathogen-
214 associated molecular pattern (PAMP)³⁹ and boosting the innate immune defence. The observed
215 decrease in the amount of eDNA in response to IL-1 β and IL-8 could impede immune defence by
216 reducing the amount of potential PAMPs.

217 In a gingival epithelial cell co-culture model, the IL-8 and IL-6 uptake efficiencies were not affected
218 by *bilRI* deletion. This observation was expected in the case of IL-6, which did not bind to BilRI *in*
219 *vitro*. The BilRI-independent uptake of IL-8 might be explained by the high concentration of IL-8 in
220 the system. For example, our organotypic gingival tissue culture system produces approximately 200
221 ng IL-8 in 24 h compared with 200 pg of IL-1 β ²⁸ during the same time period. The *A.*
222 *actinomycetemcomitans* biofilm virtually bathes in IL-8, which may allow efficient IL-8 uptake
223 without a cell surface concentrator. In our test systems, the IL-8 concentration always exceeded that
224 of IL-6. In the *in vivo* environment of periodontitis-associated biofilm, a similar surplus of IL-8 is
225 observed with approximately one hundred times more IL-8 than IL-6 in gingival crevicular fluid.⁴⁰
226 The deletion of *bilRI* exerted only minor effects on the phenotype of *A. actinomycetemcomitans*,
227 which were mainly observed as a change in the composition of the biofilm matrix. However, the
228 overexpression of BilRI caused lysis of the outer membrane. In addition, our previous study showed
229 that *E. coli* cells are more prone to cell lysis when expressing BilRI under a strong promoter.²⁴ Due to
230 the vulnerability of the outer membrane, the expression of outer membrane proteins of Gram-negative
231 bacteria needs to be precisely regulated.⁴¹ We decided to use a constitutively expressed strong *ltxP*
232 promoter instead of the endogenous *bilRI* promoter, which may be more strictly regulated, to ascertain
233 efficient complementation. Moreover, we were interested in investigating how the overproduction of
234 BilRI affects the phenotype. BilRI was not involved in binding collagen and fibrinogen, although the
235 wild-type *A. actinomycetemcomitans* cells clearly bound the proteins. Both experiments with the
236 *bilRI* mutant and purified BilRI showed similar results. Our findings are partly contradictory to those
237 obtained in previous study conducted by Bauer and co-workers,⁴² which showed that a similar protein
238 of *H. ducreyi*, which was named fibrinogen-binding protein A (FgbA), interacts with human
239 fibrinogen. The incapability of C-tagged BilRI to interact with fibrinogen cannot be explained by the

240 location of the histidine tag because N-tagged BilRI showed similar results (data not shown) and the
241 control protein FgbA, which was N-tagged, could not bind fibrinogen. More recent studies have
242 confirmed that another protein, *i.e.*, ducreyi serum resistance A (DsrA), a trimeric autotransporter, is,
243 in fact, the main binder of fibrinogen in *H. ducreyi* and that FgbA does not play a central role in
244 fibrinogen binding.⁴³ Our results are in line with those obtained in the more recent later study because
245 we also found that the slightly truncated form of FgbA, which can be found in some strains of *H.*
246 *ducreyi*, does not bind to fibrinogen. However, FgbA undoubtedly promotes *H. ducreyi* virulence;
247 thus, the major functions of FgbA and similar proteins, such as BilRI, are worth studying.
248 The differential affinity and capacity to uptake various cytokines may provide the pathogen with the
249 means to modulate the host inflammatory response and the cytokine balance. In healthy periodontal
250 tissue, IL-8 forms a concentration gradient with higher concentrations in the coronal parts of the
251 junctional epithelium, near the bacterial biofilm.⁷ During acute inflammation, neutrophils are the first
252 innate immune cells to enter the site. However, their activity, *i.e.*, the release of reactive oxygen
253 species and proteases, causes severe tissue damage if not limited by regulative actions. IL-6 signalling
254 is known to suppress chemokines, such as IL-8, which attract neutrophils and directly causes
255 neutrophil apoptosis.⁴⁴ The immune system redirects from innate to acquired immunity by replacing
256 the neutrophils with monocytes and T cells. IL-6 is involved in this process by inducing the
257 production of chemokines that attract monocytes (for a review, see ref. ⁴⁵), augmenting monocyte
258 differentiation into macrophages,⁴⁶ recruiting T cells⁴⁷ and impeding their apoptosis⁴⁸. Periodontitis
259 is characterized by progressive bone loss in tooth supportive tissues, which is associated with a high
260 receptor activator of nuclear factor κ -B (RANK) ligand (RANKL) / osteoprotegerin (OPG) ratio, *i.e.*,
261 RANKL causes bone destruction by binding RANK, which leads to the induction of osteoclast
262 production.⁴⁹ However, OPG can inhibit osteoclastogenesis by sequestering RANKL.⁵⁰ Various
263 cytokines, such as IL-1 β , IL-6, IL-11, IL-17 and TNF- α , increase the expression of RANKL over
264 OPG (for a review, see ref. ⁴⁹). IL-6 activates osteoclastogenesis together with soluble IL-6 receptor
265 (sIL-6R)⁵¹ by provoking RANKL expression⁵². Thus, high IL-6 concentration in the inflammatory
266 milieu resolves the acute inflammation reaction that is detrimental to the host tissue by enhancing the
267 clearance of neutrophils and moves the balance to acquired immunity by increasing the recruitment of

268 monocytes and T cells.⁴⁴⁻⁴⁸ However, bone homeostasis is skewed in the direction of
269 osteoclastogenesis and bone degradation due to the increased RANKL/OPG ratio.⁵² By decreasing
270 local IL-6 amounts in inflammation, *A. actinomycetemcomitans* could decelerate the clearance of
271 acute inflammation and could extend the time of the neutrophil-skewed immune reaction.
272 In conclusion, the role of intrinsically disordered BilRI is most likely to concentrate small proteins,
273 such as different host cytokines, on the surface of *A. actinomycetemcomitans*, which facilitates the
274 efficient uptake of cytokines using as yet unknown machinery. The affinity of BilRI to the cytokines
275 is relatively weak when compared with, for example, the binding of *Y. enterocolitica* YadA to
276 collagen. The weak affinity is most likely needed for the proficient transfer of the cytokine to the next
277 binding protein in the chain of internalization. Because periodontitis is an inflammatory disease
278 caused by multispecies biofilm, cytokine binding and uptake might not benefit only *A.*
279 *actinomycetemcomitans*. By binding and internalizing cytokines, *A. actinomycetemcomitans* could
280 help other species in a periodontal biofilm to persist in an inflammatory environment.⁵³ The uptake of
281 cytokines by opportunistic pathogens may disturb the balance of cytokines with low local
282 concentrations, whereas the effect on cytokines with high local concentrations, such as IL-8, might be
283 only marginal. Moreover, in low cytokine concentrations, the role of BilRI, a potential cytokine
284 concentrator, might be emphasized in facilitating the uptake of cytokines at the surface of *A.*
285 *actinomycetemcomitans*.

286 Materials and methods

287 *Cloning and expression of recombinant proteins: BilRI, FgbA, ClfA, IL-8, YadA*

288 To study the interaction of BilRI with various cytokines, the *bilRI* gene was cloned into the pET36b
289 expression vector, which inserts an 8-histidine long tag into the C-terminal end (Novagen, Darmstadt,
290 Germany) using the forward primer 5'-ATT CATATG GATGACAGCAAACTTCACC-3' and the
291 reverse primer 5'-ATA CTCGAG TTTGCTTTCAGTTTTCGC-3' during PCR. The underlined
292 sequences are the NdeI and XhoI restriction sites, respectively. The *bilRI* gene was amplified from a
293 previously produced expression vector,²⁴ which contained the gene from D7S. The plasmid was
294 transformed into bacterial cells from the BL21 CodonPlus (DE3)-RIL *E. coli* protein expression strain
295 (Stratagene, San Diego, CA, USA).

296 The recombinant BilRI containing amino acids 21-181 was expressed in Terrific broth medium (12
297 g/L tryptone, 24 g/L yeast extract, 0.4% glycerol, 17 mM KH₂PO₄, 72 mM K₂HPO₄) containing 30
298 µg/mL kanamycin. Protein expression was induced with 1 mM isopropyl β-D-1-
299 thiogalactopyranoside (IPTG) when the OD_{600nm} was 1.2. Cells were grown for 3 h under induction,
300 after which they were harvested by centrifugation (6 400×g, 10 min, 4°C), and cell pellets were stored
301 at -20°C.

302 To purify the intracellular recombinant protein, 8-10 g of cells were defrosted and suspended to 30
303 mL in binding buffer (20 mM NaH₂PO₄/Na₂HPO₄, 800 mM NaCl, 20 mM imidazole, pH 7.5)
304 including DNase I (Roche, Mannheim, Germany), 5 mM MgCl₂ and 0.2 mM phenylmethylsulfonyl
305 fluoride (PMSF) protease inhibitor. Cells were sonicated 5x15 s with a 100 Watt MSE ultrasonic
306 disintegrator. Cell debris was removed by centrifugation (48 000×g, 25 min, 4°C), and the clarified
307 supernatant containing the recombinant BilRI protein was loaded in a balanced 5-mL HisTrap HP
308 (GE Healthcare, Uppsala, Sweden) column. The unbound material was washed out with 5% elution
309 buffer (20 mM NaH₂PO₄/Na₂HPO₄, 800 mM NaCl, 500 mM Imidazole, pH 7.5), and the His-tagged
310 BilRI was eluted with 50% elution buffer. The eluate was loaded into a size-exclusion
311 chromatography Superdex 200 26/60 (GE Healthcare) column in PBS₁ (2.7 mM KCl, 1.8 mM
312 KH₂PO₄, 140 mM NaCl, and 10 mM Na₂HPO₄, pH 7.4). The recombinant BilRI does not include any

313 tryptophans or any other aromatic residues; therefore, it is nonvisible at 280 nm. However, the protein
314 could be detected in fractions based on both $A_{220\text{nm}}$ readings and Bio-Safe™ Coomassie (Bio-Rad,
315 Hercules, CA, USA)-stained SDS-PAGE (Thermo Fisher Scientific Precise™ 4-20% Tris-Glycine
316 Gels). According to the analysis, BilRI-containing protein fractions were concentrated using an
317 Amicon Ultra-15 Centrifugal Filter Unit with an Ultracel-10 membrane (Millipore, Billerica, MA,
318 USA), and the protein amount in the final concentrate was determined using the method by Lowry et
319 al.⁵⁴ Protein purity was verified with SDS-PAGE, and the homogeneity was determined by native
320 PAGE (PhastGel Gradient, 8-25, GE Healthcare).

321 Synthetic DNA with optimized codon usage for *E. coli* expression was ordered from Eurofins
322 Genomics for FgbA, including the gene for residues 20-105 from *Haemophilus ducreyi* HMC112, the
323 fibrinogen-binding segment of *Staphylococcus aureus* strain NCTC 8325 ClfA, the gene fragment for
324 residues 230-542 and the cDNA of the coding residues 23-99 of human IL-8. N-terminal NdeI and C-
325 terminal XhoI restriction sites were added for all three synthetic genes. DNA fragments were ligated
326 into the pET15b plasmid (Novagen, Darmstadt, Germany), and DNA sequences were verified with
327 sequencing.

328 FgbA was expressed, purified and identified by the same method as BilRI because it lacks all
329 aromatic residues. ClfA was expressed and purified similarly to FgbA, except the binding and elution
330 buffers contained 300 mM NaCl. The ClfA concentration was measured on a NanoDrop 2000
331 spectrophotometer (Thermo Fisher Scientific, Wilmington, DE, USA) using an $A_{280}^{0.1\%}$ of 0.999.

332 IL-8 was purified as a mature protein. The N-terminal His-tag was cut by digesting in a HisTrap
333 column with 200 NIH units of thrombin (MP Biomedicals, Santa Ana, CA, USA) at RT overnight.
334 Digested IL-8 was eluted with binding buffer, and the protein was purified from other proteins by
335 size-exclusion chromatography. After concentration with an Amicon Ultra-15 Centrifugal Filter Unit
336 with an Ultracel-10 membrane (Millipore), the protein concentration was determined with $A_{280\text{ nm}}$
337 using an $A_{280}^{0.1\%}$ of 0.863. The IL-8 molecular mass was verified with matrix-assisted laser
338 desorption/ionization time-of-flight mass spectrometry (MALDI TOF MS) (Bruker). Analysis yielded
339 a mass of 8381.99 Da (+H form) (+/-1 Da) for IL-8, whereas the theoretical mass with two cysteines

340 was 8381.67 Da, indicating that the recombinant IL-8 had 72 amino acids, suggesting that the
341 endogenous thrombin site of IL-8 was exposed.

342 The plasmid pHN-1 and the *E. coli* M15(pREP4) strain (Qiagen, Hilden, Germany) for the collagen-
343 binding fragment of *Yersinia enterocolitica* adhesin (YadA) expression were kind gifts from Professor
344 Mikael Skurnik (University of Helsinki, Finland). YadA expression and purification were performed
345 as published by Nummelin et al.⁵⁵ except that the size-exclusion chromatography buffer was PBS₁.
346 All proteins were deep-frozen with liquid nitrogen and stored at -85°C. All recombinant protein
347 preparations has high purity, as observed in the Coomassie-stained 4-20% Tris-glycine SDS-PAGE
348 gel (Fig. 7).

349 ***NMR spectroscopy studies of BilRI structure***

350 NMR spectra were collected at 298 K using either Varian INOVA 600 MHz or INOVA 800 MHz
351 NMR spectrometers (Agilent, Santa Clara, CA, USA), both equipped with cryogenically cooled ¹H,
352 ¹³C, ¹⁵N triple-resonance probeheads with z-gradient coils. For ¹H NMR spectra, measured at 600
353 MHz, the recombinant BilRI was diluted in 95%/5% H₂O/D₂O, 50 mM NaCl, pH 7 buffer in a
354 Shigemi microcell (250 µL). The final BilRI concentration was 4.6 mM. The ¹H spectrum was
355 sampled with 20,438 complex points using 64 transients per free induction decay (FID), resulting in
356 an acquisition time of 500 ms in the ¹H dimension. The two-dimensional ¹H-¹⁵N HSQC spectrum of
357 BilRI at pH 5 was measured at the 800 MHz ¹H frequency using 128 and 852 complex points in ¹⁵N
358 and ¹H dimensions, corresponding to acquisition times of 49 ms and 85.2 ms, respectively. A total of
359 256 transients per FID were used to assure sufficient signal accumulation. The total experimental time
360 was 18 h. Spectra were processed with VnmrJ (Agilent, Santa Clara, CA, USA) and analysed with
361 Sparky (T. D. Goddard and D. G. Kneller, University of California, San Francisco, CA, USA)
362 software packages.

363 ***Cytokine-binding assay for recombinant BilRI***

364 Because BilRI produced unwanted spontaneous dimers when the cysteine at position 20 was included
365 in the recombinant protein, the construct that was used in the cytokine-binding assays contains neither

366 the signal sequence (the first 19 amino acids) nor the C20. Moreover, the recombinant BilRI
367 contained an eight-histidine long tail in the C-terminus to allow detection with His-Probe (Thermo
368 Fisher Scientific).
369 A total of 100 ng of each cytokine (IL-1 β /IL-6/IL-8/IL-10/tumour necrosis factor [TNF]- α /interferon
370 [INF]- γ /transforming growth factor [TGF]- β 1) diluted in PBSN buffer (0.05% sodium azide in PBS₁)
371 was incubated in a Nunc MaxiSorp 96-well plate (Affymetrix, Santa Clara, CA, USA) at RT
372 overnight. Wells were washed three times with ion-exchanged water, after which the wells were
373 blocked with blocking buffer (0.25% BSA, 0.02% sodium azide in PBS-T) at 37°C for 3 h. The wells
374 were again washed as above, and 400 ng of C-His-tagged BilRI₂₁₋₁₈₁ was added to the wells and
375 incubated at 4°C overnight. The wells were washed four times with PBS-T using Delfia Platewash
376 (Perkin Elmer, Turku, Finland). His-Probe-HRPTM (Thermo Fisher Scientific) was diluted to 1:5000,
377 and 50 μ l of the dilution was incubated in the wells at RT for 15 min. The wells were washed again
378 four times with PBS-T as described above, and detection was performed with 2,2'-azino-bis(3-
379 ethylbenzothiazoline-6-sulfonic acid) diammonium salt (Sigma-Aldrich) in citrate buffer (10 mM
380 sodium citrate and 0.03% H₂O₂, pH 4.2). The A_{414nm} value was read using a Multiscan Go plate reader
381 (Thermo Fisher Scientific).

382 ***Collagen- and fibrinogen-binding assay for recombinant BilRI (EuLISA)***

383 The binding of BilRI to type V collagen and fibrinogen was determined in a microplate assay
384 modified from the method described by Yu et al.⁵⁶ Type V collagen from human plasma (Sigma-
385 Aldrich) was dissolved in 0.5 M acetic acid, and fibrinogen from human placenta (Sigma-Aldrich)
386 was dissolved in 0.85% NaCl at 37°C with gentle mixing for 5 h and filtered through a 0.2- μ m
387 syringe filter. Collagen and fibrinogen were diluted in PBS₁, and a total of 1 μ g of each was incubated
388 in the wells of a Nunc MaxiSorp 96-well plate (Affymetrix) at 4°C overnight. Equal amounts of BSA
389 (Sigma-Aldrich) and IL-8 (production described above) were used as negative and positive controls,
390 respectively.
391 Unbound proteins were removed by washing once with PBS₁ using a Delfia Platewash (Perkin
392 Elmer). The wells were blocked with 200 μ g of BSA in PBS₁ at RT for 1-2 h and washed as above. A

393 total of 1 μg of C-His-tagged BiRI₂₁₋₁₈₁ was diluted in Delfia Assay Buffer (Perkin Elmer) and
394 incubated in wells at RT for 1 h. YadA (0.8 μg), FgbA (1.6 μg) and ClfA (0.5 μg) were used as
395 positive collagen or fibrinogen binders. The production of these proteins is described above. The
396 wells were washed 3 times with PBS₁ using Delfia Platewash (Perkin Elmer). Then, 25 ng of
397 DELFIA® Eu-N1 Anti-6xHis antibody (Perkin Elmer) in 50 μL of Delfia Assay Buffer was incubated
398 in wells at RT for 1 h. The wells were washed as in the previous step. Detection was performed
399 measuring time-resolved fluorescence using a Victor³ multilabel plate reader (Perkin Elmer) after a 5-
400 min incubation in DELFIA® Enhancement Solution (Perkin Elmer).

401 ***Binding of IL-8 and IL-6 by the viable A. actinomycetemcomitans biofilm***

402 *A. actinomycetemcomitans* biofilms were co-cultured in a gingival mucosa model as described by
403 Paino et al.²⁸ In brief, in the model, human gingival fibroblasts (HGFs)⁵⁷ and spontaneously
404 immortalized human gingival keratinocytes (HGKs)⁵⁸ were cultured at an air-liquid interphase to
405 obtain the three-dimensional tissue organization. First, HGFs (passages 13-18) in Dulbecco's
406 modified Eagle's medium (DMEM; Gibco, Life Technologies, Paisley, UK) were suspended in
407 collagen solution (PureCol®, Advance Biomatrix, AZ, USA), and an aliquot containing 1.5×10^5
408 fibroblasts was transferred to cell culture inserts and grown for 1 day submerged in Green's
409 medium.⁵⁹ To obtain the epithelial layer in the top layer of the connective tissue, 4×10^5 HGKs
410 (passage 18-22) were added on top of the fibroblast-collagen layer. The epithelial cells were cultured
411 submerged for 1 day, and the tissue model was then lifted in the air-liquid interface and allowed to
412 mature for 5 days, after which the separately grown *A. actinomycetemcomitans* biofilm was added on
413 top of the tissue culture model. The biofilms were co-cultured with the tissue models for 24 h. Culture
414 medium was collected before and after the 24 h co-culture and stored at -80°C . In half of the cultures,
415 penicillin (63.4 IU/ml) and streptomycin (63.4 $\mu\text{g}/\text{ml}$) were used in culture media to decrease biofilm
416 viability. The co-cultures were fixed with 10% formalin solution overnight, and the sectioning of
417 paraffin-embedded samples was performed using standard histological techniques.
418 Before staining with anti-IL-8 and anti-IL-6 antibodies, the specimens were mechanically
419 deparaffinized, and heat-mediated antigen retrieval was conducted in 10 mM citrate buffer (pH 6.0)

420 with microwaving. The staining was performed with Dako TechMate™ 500 Plus Autostainer (Dako,
421 Glostrup, Denmark) using 20 µg/mL of primary polyclonal rabbit IgG against IL-8 (NBP2-16958;
422 Novus Biologicals, Cambridge, UK) and IL-6 (NBP2-16957; Novus Biologicals) and a Dako
423 REAL™ Detection System, Peroxidase/DAB+, Rabbit/Mouse (Code K5001; Dako) as instructed by
424 the producer. The histological samples were imaged with Leica DM RXA light microscope using
425 Leica HC PL APO 20x / 0.70 objective.

426 The culture media samples collected prior to the co-culture indicating the basal level of cytokine
427 expression, along with the samples collected after 24 h co-culture, were analysed with IL-8- and IL-6-
428 specific enzyme-linked immunosorbent assay (ELISA) kits (SABiosciences, Qiagen, Germantown,
429 MD, USA). Because the volume of the medium varied slightly between different experiments, the
430 amount of cytokine that was excreted into the medium was calculated as a total amount (ng) leaked
431 into the culture medium in 24 h.

432 ***Prediction of the size of the mRNA expressing BilRI***

433 The Prokaryotic Operon Database (ProOpDB, <http://operons.ibt.unam.mx/OperonPredictor>)³⁰ was
434 used to predict whether *bilRI* is a stand-alone gene or belongs to an operon. Because *A.*
435 *actinomycetemcomitans* strain D7S was not deposited into the database, *A. actinomycetemcomitans*
436 strain D11S was used. The hypothetical protein D11S_0933 of *A. actinomycetemcomitans* D11S-1
437 (GenBank accession number CP001733.1) has an identical amino acid sequence to the BilRI protein
438 of *A. actinomycetemcomitans* D7S. In addition, the genes surrounding the gene encoding BilRI are
439 similar in both strains. Downstream of *bilRI* is a gene encoding septum site-determining protein
440 MinC, whereas genes encoding the SixA phosphohistidine phosphatase, phosphoglucosamine mutase
441 and dihydropteroate synthase are found upstream of *bilRI*.

442 ***Markerless bilRI-deletion mutant***

443 A single-gene-deletion mutant of *bilRI* was produced from *A. actinomycetemcomitans* strain D7S.⁶⁰
444 The strain was recovered from -80°C frozen storage cultures by culturing on modified tryptone soy
445 agar (TSA) plates consisting of 3 % tryptone soy broth (TSB, Lab-M, Lancashire, UK), 0.3 % yeast
446 extract (Lab-M), 1.5 % agar and 5 % heat-inactivated horse serum (HyClone, SH30074.03, Thermo

447 Fisher Scientific) in a candle jar at 37°C for 2.5 days. In addition, two types of TSB media were used.
448 TSB₁ contained 3 % TSB and 0.6 % yeast extract. TSB₂ was additionally supplemented with 0.8%
449 separately autoclaved glucose. Whenever necessary, the cultures were supplemented with the
450 appropriate antibiotics: either 50 µg/mL spectinomycin or 6 µg/mL tetracycline.
451 The plasmids used for mutant generation were generous gifts from Professor Casey Chen (University
452 of Southern California, Los Angeles, CA, USA). The pLox2-Spe plasmid contained a *spe* cassette
453 flanked by *loxP* sites.⁶¹ The pAT-Cre plasmid contained the *cre* recombinase and *tet(O)* genes.^{62, 63}
454 The plasmids were amplified in *Escherichia coli* strain TOP10 (Invitrogen).
455 The gene encoding BilRI (NC_017846.1 AaD7S_02241) was deleted using the Cre-*loxP* mediated
456 recombination method optimized for *A. actinomycetemcomitans*.^{61, 62} The primer sequences used for
457 PCR product generation in the target-gene-deletion mutant are listed in Table 1. First, a 2960-bp PCR
458 product containing the *bilRI* gene was amplified from the genome of *A. actinomycetemcomitans* D7S
459 using bilRI_nest primers. The PCR product was then used to generate two PCR fragments flanking
460 the *bilRI* gene in both the downstream and upstream directions. The primer pair
461 ycgL_FD/bilRI_RD_BamHI was used to amplify the downstream region, and primer pair phoGlu-
462 R/sixA_FD_SalI was used for the upstream region. The PCR fragments and pLox2-spe-plasmid were
463 digested with BamHI and/or SalI restriction enzymes (FastDigest restriction enzymes, Thermo Fisher
464 Scientific). After fragment isolation, the ligation was completed by incubating the amplicons and the
465 *spe*-cassette fragment (130 ng each) in the presence of T4 DNA ligase (Thermo Fisher Scientific).
466 The natural transformation was performed according to a previously described method.^{60, 64} In brief,
467 suspensions of plate-grown *A. actinomycetemcomitans* cells were prepared in TSB₁, and the bacterial
468 cell number was estimated according to the method described by Karched et al.³¹ Then, 2×10⁷ colony-
469 forming units (CFUs) were plated on TSA-plates, and the cells were grown in a candle jar at 37°C for
470 2 h after mixing the recipient cells with the ligation mix (250 ng of DNA). After culturing for 5 h, the
471 cells were scraped off the plate, resuspended in 150 µL of TSB₁ and plated on a spectinomycin-
472 supplemented TSA plate. Colony PCR was used to confirm the presence of a deletion in the *bilRI*
473 gene site in the *A. actinomycetemcomitans* D7S genome. Using this method, a loopful of bacteria was

474 suspended in lysis buffer (20 µg/mL proteinase K, 2.5% glycerol in 10 mM Tris-HCl, pH 8.0).
475 Twenty microliters of the resulting suspension were added to a PCR reaction using bilRI_nest-
476 primers, and the correct 3550-bp PCR product was detected. The pAT-Cre plasmid was then
477 transformed into electrocompetent primary *bilRI*-deletion mutant cells by electroporation (5 ms, 1250
478 V) using a BTV ECM399 electroporation apparatus (BTX Instrument Division, Harvard Apparatus,
479 Inc., Holliston, MA, USA) to remove the *spe*-cassette. After culturing the cells in TSB₂ for 2 h, the
480 cells were plated on TSA-plates supplemented with tetracycline and grown for a few days until visible
481 colonies were formed. The selected colonies were further plated onto TSA-plates with no antibiotics
482 and with tetracycline and spectinomycin and then grown for 4 days. Colonies sensitive to both
483 antibiotics were considered potential markerless *bilRI* mutants. Colony PCR using minc_F_1 (5'-
484 CGCGCTATCAACCGACTAAA-3') and SixA_R_2 primers (5'-TTTATCTCGGTGATGAGCGC-
485 3') was used to select products of the correct size (2100 bp), and the products were further verified by
486 sequencing the flanking regions of the *bilRI* gene in both directions by Eurofins Genomics
487 (Ebersberg, Germany). Moreover, the absence of *bilRI* in the *bilRI* mutant was verified by PCR using
488 genomic DNA as the template and primers²⁴ that amplify the whole *bilRI* gene, including the signal
489 sequence.

490 ***Restoration of BilRI expression in the bilRI-deletion mutant***

491 Because we did not succeed in restoring the *bilRI* gene to the markerless *bilRI* deletion mutant despite
492 many attempts, we decided to restore BilRI expression using an *A. actinomycetemcomitans*/*E. coli*
493 shuttle plasmid under a constitutively expressed leucotoxin promoter (*ltxP*). The *bilRI* gene was
494 amplified from *A. actinomycetemcomitans* strain D7S by PCR using the 5'-
495 ATACTCGAGTTTAGGAGTAACGATG-3' forward primer and the 5'-
496 TTTCTGCAGTTATTTGCTTTCAGTT-3' reverse primer, which contained XhoI and PstI restriction
497 sites, respectively. The *bilRI* gene was inserted into *ltxP* from the pVT1296 plasmid⁶⁵ by ligating the
498 *bilRI* PCR product into XhoI- and PstI-digested pVT1296. The final *ltxP-bilRI* construct was moved
499 to the pPK1-based⁶⁶ pVT1503 plasmid⁶⁷ by cutting the pVT1296-based construct with PstI, blunting
500 the ends with Klenow, cutting *ltxP-bilRI* from the plasmid with KpnI, and ligating *ltxP-bilRI* to KpnI-

501 and EcoRV-digested pVT1503 (KanR). The correct insert size was confirmed through KpnI-EcoRI
502 double digestion of the final expression plasmid pVT1503-*ltxP-bilRI*. The *bilRI*-containing product of
503 the KpnI-EcoRI-digested expression plasmid pVT1503-*ltxP-bilRI* was ligated into the KpnI-EcoRI-
504 digested pUC19 plasmid (New England Biolabs, Ipswich, MA, USA) and sequenced (Eurofins
505 Genomics). The expression plasmid pVT1503-*ltxP-bilRI* was then transformed into a markerless
506 *bilRI*-deletion mutant through natural transformation as described above. This time, 300 ng of DNA
507 was mixed with cells and supplemented with 1 mM CaCl₂ to improve the transformation efficiency.⁶⁸
508 After incubation, the transformants were screened on TSA plates supplemented with 30 µg/mL
509 kanamycin to select a BilRI-overexpressing variant containing the pVT1503-based expression
510 plasmid.

511 ***Effect of BilRI on biofilm formation***

512 *A. actinomycetemcomitans* D7S wild-type, *bilRI* mutant and BilRI-overexpressing strains were
513 compared to determine the effect of BilRI on biofilm formation, which was measured through crystal
514 violet staining.³² Briefly, *A. actinomycetemcomitans* D7S wild-type and *bilRI* strains were grown on
515 TSA-blood-plates (37 g/L TSA [Lab-M], 3 g/L agar, 5% defibrinated sheep blood) in a candle jar at
516 37°C for three days. A uniform cell suspension was prepared from plate-grown bacteria in TSB₂
517 medium, and the cell density was determined by measuring the optical density.³¹ The cell suspension
518 was added to the wells of a 48-well microtitre plate such that each well contained 2.5x10⁷ CFUs in a
519 total volume of 0.5 mL. Seven replicates of each strain were prepared. The plate was incubated in a
520 candle jar at 37°C overnight. The medium was removed with suction, 200 µL of Gram-staining
521 reagent (20 mg/mL crystal violet, 8 mg/mL ammonium oxalate, and 20% ethanol) was added to each
522 well, and the samples were incubated at RT for 10 min. The Gram stain was removed with suction,
523 and the wells were washed seven times with ultrapure water. After 200 µL of 95% ethanol was added
524 to the wells, the plates were incubated at RT for 10 min. The amount of released stain was measured
525 by transferring 100 µL of liquid from each well to a 96-well microtitre plate, and the A_{620nm} value was
526 measured using a Multiscan Go plate reader (Thermo Fisher Scientific).

527 ***Effect of BilRI on biofilm composition***

528 Because the *bilRI* mutant formed similar amounts of biofilm as the wild-type *A.*
529 *actinomycetemcomitans* strain, we further analysed the biofilm composition of the wild-type and
530 *bilRI* mutant strains. However, because the *bilRI* mutant in which BilRI expression was restored with
531 a plasmid loses its viability when expressing elevated amounts of the outer membrane protein BilRI
532 (Figs. 4A-4D), its biofilm composition could not be studied. Biofilm cultures were generated as
533 described above with the exception that the biofilms were grown in 50-mL cell culture bottles
534 (Cellstar #690160, Greiner Bio-One, Frickenhausen, Germany) by adding 2.5×10^8 CFUs in a total
535 volume of 5 mL of TSB₂ medium. The biofilms were grown in a candle jar at 37°C overnight.
536 Samples were collected from the culture medium and cultured on blood agar plates to ensure that the
537 biofilms were not contaminated. The TSB₂ medium was removed, the biofilms were washed three
538 times with 10 mL of PBS₁, and the biofilm was scraped into 3 mL of PBS₁ with an inoculation loop.
539 The samples were divided into three 1-mL aliquots, the biofilm mass of centrifuged (12,000×g, 15
540 min) pellets from each sample was weighed, and the amounts of total protein and eDNA were
541 estimated using the methods described below.
542 For the total protein measurement, the pre-weighed biofilm pellets were suspended in 200 µL of
543 ultrapure water with mild sonication (2×5 s, 5-µm amplitude, 100-Watt MSE ultrasonic disintegrator),
544 and the volume was then doubled by adding sodium dodecyl sulphate (SDS) to a final concentration
545 of 2% in 0.5× PBS₁. The samples were boiled for 10 min, the insoluble fraction was separated through
546 a short centrifugation, and the total protein amount in the supernatant was measured using the method
547 described by Lowry et al.⁵⁴
548 For eDNA extraction,⁶⁹ the pre-weighed biofilm pellet was suspended in 0.9% NaCl to obtain 9
549 mg/mL, and the suspension was homogenized using mild sonication, as described above. The
550 suspension was supplemented with 1× Glyko Buffer 2 (New England Biolabs) and 250 units of
551 PNGase F (New England Biolabs). After the mixture was incubated at 37°C for 30 min, proteinase K
552 (Thermo Fisher Scientific) was added to a final concentration of 5 µg/mL, the samples were incubated
553 at 37°C for 30 min. The samples were filtered through a 0.2-µm polyethersulfone (PES) membrane
554 (VWR) before the amount of eDNA was determined with propidium iodide, as described by Rose et

555 al.⁷⁰ Briefly, 25 μ L of biofilm extract was mixed with an equal volume of 6 μ M propidium iodide in a
556 white 96-well plate (Thermo Fisher Scientific). The plate was incubated in the dark at RT for 15 min
557 before the fluorescence was read using a Hidex Sense Microplate reader (Hidex, Turku, Finland) with
558 a 535-nm excitation filter and a 620-nm emission filter.

559 ***Binding of bilRI mutant cells on collagen and fibrinogen***

560 The binding of *A. actinomycetemcomitans* to type V collagen and fibrinogen was determined using a
561 microplate assay modified from the methods described by Yu et al.⁵⁶ and Tang and Mintz⁷¹. Collagen
562 and fibrinogen solutions were prepared as in the collagen- and fibrinogen-binding assay for
563 recombinant BilRI. A total of 1 μ g of collagen in sodium bicarbonate buffer (16 mM sodium
564 carbonate, 34 mM sodium bicarbonate, and 0.02% sodium azide, pH 9.6) or 25 ng of fibrinogen in
565 PBSN₁ (0.05% sodium azide in PBS₁) was added to the wells of a Nunc MaxiSorp 96-well plate
566 (Affymetrix). The plate was coated at 4°C overnight. Liquid was removed from the wells by
567 decanting, and the wells were washed four times with ion-exchanged water. The wells were blocked
568 with 1 mg of BSA in PBS₁ at RT for 2 h, and the wells were then washed as described above. Wild-
569 type *A. actinomycetemcomitans* and the *bilRI* mutant were collected from TSA-blood plates, a
570 uniform bacterial suspension in PBS₁ was prepared, and the number of bacterial cells was estimated as
571 described above. One hundred microliters of bacterial suspension (1.25x10⁶, 2.5x10⁶, 5x10⁶ and 1x10⁷
572 CFUs) were added, and the mixture was incubated in a candle jar at 37°C for 1 h. After the liquid was
573 removed from the wells by suction, the plate was washed three times with 200 μ L of PBS-T (PBS₁
574 with 0.05% Tween-20). A volume of 100 μ L of anti-serotype A antibody⁷² (1/1000, diluted in PBS-T
575 supplemented with 0.25% BSA) was added to each well, and the plate was incubated at RT for 1 h.
576 The wells were washed four times with PBS-T using a Delfia Platewash (Perkin Elmer). After 100 μ L
577 of anti-rabbit IgG-horseradish peroxidase (HRP) antibody (Promega, 1/9000, diluted into PBS-T) was
578 added to each well, the plate was incubated at RT for 1 h. The wells were washed as in the previous
579 step, and detection was conducted as in the investigation of BilRI binding to cytokines but measured
580 at A_{405nm}.

581 ***Role of BilRI in the binding and internalization of IL-8 and IL-6 by the biofilm cells***

582 A clinical wild-type *A. actinomycetemcomitans* strain D7S, the *bilRI* mutant strain and the BilRI-
583 overexpressing strain were revived from frozen milk stocks or TSB₂ containing 20% glycerol through
584 growth on TSA-blood plates for 4 days. Bacterial suspensions were prepared in TSB₂ medium, and
585 the number of bacterial cells was estimated as described above. Then, 2.5 mL of suspension (5×10^8
586 CFUs) was added to sterile hydrophilic PES membranes (Supor®-200; diameter of 25 mm; 0.2- μ m
587 pore size; Pall Corporation, Ann Arbor, MI, USA) in a 6-well culture plate followed by incubation in
588 a candle jar at 37°C for 24 h. To remove non-adherent bacteria, the membranes were briefly washed
589 twice with 0.85% NaCl prior to a 24-h incubation in RPMI-1640 medium (Sigma-Aldrich)
590 supplemented with 0.6 g/L L-glutamine (Sigma-Aldrich).

591 In parallel to biofilm formation, spontaneously immortalized HGKs⁵⁸ were maintained in
592 keratinocyte SFM growth medium (#17005-075, Gibco®, Thermo Fisher Scientific, Paisley, UK)
593 containing the supplement provided by the manufacturer. Briefly, the HGKs (passages 12-16) were
594 grown to confluence in 175-cm² cell culture flasks with a medium change every 4–5 days. The same
595 day on which the biofilms were incubated with RPMI-1640 medium, the confluent epithelial cells in
596 flasks were reseeded into six-well plates (4×10^5) and grown for 24 h. Prior to co-culturing, the
597 biofilms were gently washed with PBS₂ (10 mM Na₂HPO₄ and 150 mM NaCl, pH 7.4). Then, the
598 biofilms were placed on top of HGKs, and the co-cultures were incubated at 37°C in 5% CO₂ for 24 h.
599 After the co-culture with gingival epithelial cells, the biofilms were fixed initially in 4 %
600 paraformaldehyde with 2.5 % sucrose in 0.1 M phosphate buffer pH 7.4 at RT for 6 h. Then, the
601 biofilms were moved to 4°C, and an extra 1-h fixation was applied in the same fixative. After the
602 fixation was completed, the co-cultures were stored in 2.3 M sucrose in PBS₂ at 4°C. For immuno-
603 electron microscopy (immuno-EM) detection, small spherical samples (with a diameter of 2 mm)
604 were taken from the co-cultures using a biopsy punch (Miltex, Lake Success, NY, USA).

605 The immuno-EM detection of IL-1 β , IL-8 and IL-6 in the spherical biofilm samples was performed as
606 described previously.²⁸ Briefly, the samples were stored in 2.3 M PBS₂ at 4°C before freezing in
607 liquid nitrogen and cryosectioning. The sections were incubated in 0.2% gelatin-PBS₂ followed by
608 0.1% glycine-PBS₂. The primary antibodies, rabbit anti-IL-1 β (NB600-633; Novus Biologicals),
609 rabbit anti-IL-8 (NBP2-16958; Novus Biologicals), and rabbit anti-IL-6 (NBP2-16957), were diluted

610 in 1% BSA-PBS₂ and incubated with the samples for 60 min. After washing with 1% BSA-PBS₂, the
611 bound antibodies were detected by incubating with protein A-gold complex (10 nm) diluted in 0.1%
612 BSA-PBS₂.⁷³ Negative controls were prepared similarly, except primary antibodies were omitted from
613 the protocol. The labelled sections were embedded in methylcellulose and examined with a Philips
614 CM100 transmission electron microscope (FEI Company, Eindhoven, The Netherlands). Two
615 independent repetitions of the experiments were performed, of which the amounts of gold labels in
616 39-104 labelled cells were counted from 9-18 representative pictures.

617 *Effect of IL-1 β and IL-8 on biofilm composition of A. actinomycetemcomitans*

618 Because it was impossible to control the amounts of cytokines in the organotypic mucosa co-culture
619 model, we studied the effects of IL-1 β and IL-8 on the composition of the biofilm matrix by exposing
620 *A. actinomycetemcomitans* biofilms to similar amounts (10 ng/mL) of recombinant cytokines in 50-
621 mL tissue culture bottles or 48-well standard tissue culture-treated plates.

622 *A. actinomycetemcomitans* D7S wild-type and *bilRI* mutant strains were grown on TSA-blood plates
623 for four days. An even cell suspension was prepared in TSB₂ medium, and the number of bacterial
624 cells was estimated as described above. The cell suspension was added to 50-mL cell culture bottles
625 (Cellstar #690160, Greiner Bio-One, Frickenhausen, Germany) to obtain a cell density of 1×10^9 CFUs
626 in 5 mL of TSB₂. After a 5-h incubation in a candle jar at 37°C, the medium was discarded, and the
627 attached biofilms were washed with 9 mL of RPMI-1640 medium (Sigma-Aldrich) supplemented
628 with 0.6 g/L L-glutamine (Sigma-Aldrich). Five millilitres of the same medium was added to the
629 culture bottles and supplemented with 10 ng/mL IL-1 β or IL-8. One bottle per strain was prepared
630 without cytokines as a control. The biofilms were grown in a candle jar overnight at 37°C. The
631 following morning, the medium was replaced by fresh medium supplemented with 10 ng/mL
632 cytokines when needed. The biofilms were grown for an additional 5 h and then collected as described
633 above. The eDNA and protein amounts in the biofilms were determined from pre-weight cell pellets
634 as described above.

635 To determine the effect of cytokines on the PGA amount and total biofilm formation, biofilms were
636 prepared using a protocol similar to that described above with the exception that they were grown on a

637 48-well microtiter plate instead of culture bottles and 3.8×10^7 CFUs were added to each well. Each
638 sample was prepared in triplicate. After the biofilms were grown for 5 h in TSB₂ and for 22 h in
639 RPMI-1640 (supplemented with L-glutamine and cytokines as described above), the biofilms were
640 washed with ultrapure water and stained with Congo red to determine the PGA amount in the biofilms
641 using the method described by Izano et al.¹⁶ with some modifications. Briefly, the biofilms were
642 stained with 200 μ L of 1% Congo red dye (Sigma-Aldrich) diluted in ultrapure water. The stain was
643 incubated for 2 min, and the wells were washed twice with ultrapure water. The bound dye was
644 solubilized with 200 μ L of 50% DMSO (Sigma-Aldrich) at RT for 1 h. The absorbance was measured
645 using a Multiscan GO plate reader (Thermo Fisher Scientific) at 405 nm. To determine the overall
646 biofilm formation, identically prepared biofilms were alternatively stained with Crystal violet stain as
647 described above.

648 ***Statistics***

649 The binding of recombinant BilRI to various cytokines was analysed through related-samples
650 Friedman's two-way analysis of variance on ranks, and this was followed by an analysis of BilRI
651 binding to IL-8 through a paired-samples T-test (IBM SPSS Statistics 22). Due to the small sample
652 size, which was always less than ten, the differences in the biofilm composition, binding capacities
653 and uptake efficiencies of various cytokines of wild-type and *bilRI* mutant strains were analysed
654 using the nonparametric Mann-Whitney U-test (IBM SPSS Statistics 22). The effects of cytokines on
655 the biofilm amount and composition were analysed using a Kruskal-Wallis test followed by paired
656 Mann-Whitney U-tests with Bonferroni corrections (IBM SPSS Statistics 22) when needed.
657 Differences were regarded as statistically significant at $p < 0.05$.

658 Acknowledgements

659 This work was supported by the Academy of Finland grants 265609 and 272960 to RI and 288235 to
660 PP and the Central Foundation of Finnish Cultural Foundation to TA. Keith P. Mintz is acknowledged
661 for kindly providing pVT1296 and pVT1503 plasmids. Mrs Katja Sampalahti, Mrs Mariia Valkama
662 and Mrs Marja-Riitta Uola are thanked for their skilful technical assistance in tissue culture and
663 immunohistological staining. MSc Kalle Sipilä is thanked for help in the EuLISA analysis and Ms
664 Nelli Vahvelainen for assistance in analysing the biofilm composition. The immuno-EM studies were
665 performed at the EM laboratory of Biocenter Oulu, University of Oulu, Finland. The light
666 microscopic imaging was performed at the Cell Imaging Core (Turku Centre for Biotechnology,
667 University of Turku and Åbo Akademi University).

668 Disclosure of potential conflicts of interest

669 The authors declare no potential conflicts of interests.

670 References

- 671 [1] Uversky VN. Intrinsically disordered proteins from A to Z. *Int J Biochem Cell Biol* 2011;
672 43:1090-103; PMID: 21501695; DOI: 10.1016/j.biocel.2011.04.001 [doi].
- 673 [2] Tompa P, Dosztanyi Z, Simon I. Prevalent structural disorder in *E. coli* and *S. cerevisiae*
674 proteomes. *J Proteome Res* 2006; 5:1996-2000; PMID: 16889422; DOI: 10.1021/pr0600881
675 [doi].
- 676 [3] Wright PE, Dyson HJ. Intrinsically disordered proteins in cellular signalling and regulation.
677 *Nat Rev Mol Cell Biol* 2015; 16:18-29; PMID: 25531225; DOI: 10.1038/nrm3920 [doi].
- 678 [4] Zambon JJ. *Actinobacillus actinomycetemcomitans* in human periodontal disease. *J Clin*
679 *Periodontol* 1985; 12:1-20; PMID: 3882766.
- 680 [5] Haffajee AD, Socransky SS. Microbial etiological agents of destructive periodontal
681 diseases. *Periodontol* 2000 1994; 5:78-111.
- 682 [6] Teles RP, Gursky LC, Faveri M, Rosa EA, Teles FR, Feres M, Socransky SS, Haffajee AD.
683 Relationships between subgingival microbiota and GCF biomarkers in generalized
684 aggressive periodontitis. *J Clin Periodontol* 2010; 37:313-23; PMID: 20447254; DOI:
685 10.1111/j.1600-051X.2010.01534.x; 10.1111/j.1600-051X.2010.01534.x.
- 686 [7] Darveau RP. Periodontitis: A polymicrobial disruption of host homeostasis. *Nat Rev*
687 *Microbiol* 2010; 8:481-90; PMID: 20514045; DOI: 10.1038/nrmicro2337.
- 688 [8] Haubek D, Johansson A. Pathogenicity of the highly leukotoxic JP2 clone of
689 *Aggregatibacter actinomycetemcomitans* and its geographic dissemination and role in
690 aggressive periodontitis. *J Oral Microbiol* 2014; 6:10.3402/jom.v6.23980. eCollection 2014;
691 PMID: 25206940; DOI: 10.3402/jom.v6.23980 [doi].
- 692 [9] Hajishengallis G. The inflammophilic character of the periodontitis-associated microbiota.
693 *Mol Oral Microbiol* 2014; 29:248-57; PMID: 24976068; DOI: 10.1111/omi.12065 [doi].
- 694 [10] Bosshardt DD, Lang NP. The junctional epithelium: From health to disease. *J Dent Res*
695 2005; 84:9-20; PMID: 15615869.

- 696 [11] Hyvärinen K, Mäntylä P, Buhlin K, Paju S, Nieminen MS, Sinisalo J, Pussinen PJ. A
697 common periodontal pathogen has an adverse association with both acute and stable
698 coronary artery disease. *Atherosclerosis* 2012; 223:478-84; PMID: 22704805; DOI:
699 10.1016/j.atherosclerosis.2012.05.021; 10.1016/j.atherosclerosis.2012.05.021.
- 700 [12] Kozarov EV, Dorn BR, Shelburne CE, Dunn WA, Jr, Progulske-Fox A. Human
701 atherosclerotic plaque contains viable invasive *Actinobacillus actinomycetemcomitans* and
702 *Porphyromonas gingivalis*. *Arterioscler Thromb Vasc Biol* 2005; 25:e17-8; PMID:
703 15662025; DOI: 10.1161/01.ATV.0000155018.67835.1a.
- 704 [13] Das M, Badley AD, Cockerill FR, Steckelberg JM, Wilson WR. Infective endocarditis
705 caused by HACEK microorganisms. *Annu Rev Med* 1997; 48:25-33; PMID: 9046942; DOI:
706 10.1146/annurev.med.48.1.25 [doi].
- 707 [14] Rahamat-Langendoen JC, van Vonderen MG, Engström LJ, Manson WL, van Winkelhoff
708 AJ, Mooi-Kokenberg EA. Brain abscess associated with *Aggregatibacter*
709 *actinomycetemcomitans*: Case report and review of literature. *J Clin Periodontol* 2011;
710 38:702-6; PMID: 21539594; DOI: 10.1111/j.1600-051X.2011.01737.x [doi].
- 711 [15] Donlan RM, Costerton JW. Biofilms: Survival mechanisms of clinically relevant
712 microorganisms. *Clin Microbiol Rev* 2002; 15:167-93; PMID: 11932229.
- 713 [16] Izano EA, Sadvskaya I, Wang H, Vinogradov E, Ragnath C, Ramasubbu N, Jabbouri S,
714 Perry MB, Kaplan JB. Poly-N-acetylglucosamine mediates biofilm formation and detergent
715 resistance in *Aggregatibacter actinomycetemcomitans*. *Microb Pathog* 2008; 44:52-60;
716 PMID: 17851029; DOI: 10.1016/j.micpath.2007.08.004.
- 717 [17] Inoue T, Shingaki R, Sogawa N, Sogawa CA, Asami J, Kokeguchi S, Fukui K. Biofilm
718 formation by a fimbriae-deficient mutant of *Actinobacillus actinomycetemcomitans*.
719 *Microbiol Immunol* 2003; 47:877-81; PMID: 14638999.
- 720 [18] Kachlany SC, Planet PJ, Desalle R, Fine DH, Figurski DH, Kaplan JB. Flp-1, the first
721 representative of a new pilin gene subfamily, is required for non-specific adherence of
722 *Actinobacillus actinomycetemcomitans*. *Mol Microbiol* 2001; 40:542-54; PMID: 11359562;
723 DOI: mmi2422 [pii].

- 724 [19] Schreiner HC, Sinatra K, Kaplan JB, Furgang D, Kachlany SC, Planet PJ, Perez BA,
725 Figurski DH, Fine DH. Tight-adherence genes of *Actinobacillus actinomycetemcomitans*
726 are required for virulence in a rat model. *Proc Natl Acad Sci U S A* 2003; 100:7295-300;
727 PMID: 12756291; DOI: 10.1073/pnas.1237223100.
- 728 [20] Wang Y, Chen C. Mutation analysis of the flp operon in *Actinobacillus*
729 *actinomycetemcomitans*. *Gene* 2005; 351:61-71; PMID: 15837433; DOI:
730 10.1016/j.gene.2005.02.010.
- 731 [21] Wu L, Estrada O, Zaborina O, Bains M, Shen L, Kohler JE, Patel N, Musch MW, Chang
732 EB, Fu YX, et al. Recognition of host immune activation by *Pseudomonas aeruginosa*.
733 *Science* 2005; 309:774-7; PMID: 16051797; DOI: 10.1126/science.1112422.
- 734 [22] Zav'yalov VP, Chernovskaya TV, Navolotskaya EV, Karlyshev AV, MacIntyre S, Vasiliev
735 AM, Abramov VM. Specific high affinity binding of human interleukin 1 beta by Caf1A
736 usher protein of *Yersinia pestis*. *FEBS Lett* 1995; 371:65-8; PMID: 7664886; DOI: 0014-
737 5793(95)00878-D [pii].
- 738 [23] Mahdavi J, Royer PJ, Sjölander HS, Azimi S, Self T, Stoof J, Wheldon LM, Brännström K,
739 Wilson R, Moreton J, et al. Pro-inflammatory cytokines can act as intracellular modulators
740 of commensal bacterial virulence. *Open Biol* 2013; 3:130048; PMID: 24107297; DOI:
741 10.1098/rsob.130048 [doi].
- 742 [24] Paino A, Ahlstrand T, Nuutila J, Navickaite I, Lahti M, Tuominen H, Välimaa H,
743 Lamminmäki U, Pöllänen MT, Ihalin R. Identification of a novel bacterial outer membrane
744 interleukin-1Beta-binding protein from *Aggregatibacter actinomycetemcomitans*. *PLoS One*
745 2013; 8:e70509; PMID: 23936223; DOI: 10.1371/journal.pone.0070509;
746 10.1371/journal.pone.0070509.
- 747 [25] McLaughlin RA, Hoogewerf AJ. Interleukin-1beta-induced growth enhancement of
748 *Staphylococcus aureus* occurs in biofilm but not planktonic cultures. *Microb Pathog* 2006;
749 41:67-79; PMID: 16769197; DOI: S0882-4010(06)00058-1 [pii];
750 10.1016/j.micpath.2006.04.005 [doi].

- 751 [26] Paino A, Tuominen H, Jääskeläinen M, Alanko J, Nuutila J, Asikainen SE, Pelliniemi LJ,
752 Pöllänen MT, Chen C, Ihalin R. Trimeric form of intracellular ATP synthase subunit beta of
753 *Aggregatibacter actinomycetemcomitans* binds human interleukin-1beta. *PLoS One* 2011;
754 6:e18929; PMID: 21533109; DOI: 10.1371/journal.pone.0018929.
- 755 [27] Kanangat S, Postlethwaite A, Cholera S, Williams L, Schaberg D. Modulation of virulence
756 gene expression in *Staphylococcus aureus* by interleukin-1beta: Novel implications in
757 bacterial pathogenesis. *Microbes Infect* 2007; 9:408-15; PMID: 17307379; DOI:
758 10.1016/j.micinf.2006.12.018.
- 759 [28] Paino A, Lohermaa E, Sormunen R, Tuominen H, Korhonen J, Pöllänen MT, Ihalin R.
760 Interleukin-1beta is internalised by viable *Aggregatibacter actinomycetemcomitans* biofilm
761 and locates to the outer edges of nucleoids. *Cytokine* 2012; 60:565-74; PMID: 22898394;
762 DOI: 10.1016/j.cyto.2012.07.024.
- 763 [29] Hellman M, Tossavainen H, Rappu P, Heino J, Permi P. Characterization of intrinsically
764 disordered prostate associated gene (PAGE5) at single residue resolution by NMR
765 spectroscopy. *PLoS One* 2011; 6:e26633; PMID: 22073178; DOI:
766 10.1371/journal.pone.0026633 [doi].
- 767 [30] Taboada B, Ciria R, Martinez-Guerrero CE, Merino E. ProOpDB: Prokaryotic operon
768 DataBase. *Nucleic Acids Res* 2012; 40:D627-31; PMID: 22096236; DOI:
769 10.1093/nar/gkr1020 [doi].
- 770 [31] Karched M, Paul-Satyaseela M, Asikainen S. A simple viability-maintaining method
771 produces homogenic cell suspensions of autoaggregating wild-type *Actinobacillus*
772 *actinomycetemcomitans*. *J Microbiol Methods* 2007; 68:46-51; PMID: 16904783; DOI:
773 S0167-7012(06)00190-4 [pii]; 10.1016/j.mimet.2006.06.004 [doi].
- 774 [32] Kaplan JB, Meyenhofer MF, Fine DH. Biofilm growth and detachment of *Actinobacillus*
775 *actinomycetemcomitans*. *J Bacteriol* 2003; 185:1399-404; PMID: 12562811.
- 776 [33] Tompa P, Schad E, Tantos A, Kalmar L. Intrinsically disordered proteins: Emerging
777 interaction specialists. *Curr Opin Struct Biol* 2015; 35:49-59; PMID: 26402567; DOI:
778 S0959-440X(15)00124-4 [pii].

- 779 [34] Oscarsson J, Karched M, Thay B, Chen C, Asikainen S. Proinflammatory effect in whole
780 blood by free soluble bacterial components released from planktonic and biofilm cells. *BMC*
781 *Microbiol* 2008; 8:206; PMID: 19038023; DOI: 10.1186/1471-2180-8-206.
- 782 [35] Okshevsky M, Meyer RL. The role of extracellular DNA in the establishment, maintenance
783 and perpetuation of bacterial biofilms. *Crit Rev Microbiol* 2015; 41:341-52; PMID:
784 24303798; DOI: 10.3109/1040841X.2013.841639 [doi].
- 785 [36] Chiang WC, Nilsson M, Jensen PO, Hoiby N, Nielsen TE, Givskov M, Tolker-Nielsen T.
786 Extracellular DNA shields against aminoglycosides in *Pseudomonas aeruginosa* biofilms.
787 *Antimicrob Agents Chemother* 2013; 57:2352-61; PMID: 23478967; DOI:
788 10.1128/AAC.00001-13 [doi].
- 789 [37] Jones EA, McGillivray G, Bakaletz LO. Extracellular DNA within a nontypeable
790 *Haemophilus influenzae*-induced biofilm binds human beta defensin-3 and reduces its
791 antimicrobial activity. *J Innate Immun* 2013; 5:24-38; PMID: 22922323; DOI:
792 10.1159/000339961 [doi].
- 793 [38] Peterson BW, van der Mei HC, Sjollem J, Busscher HJ, Sharma PK. A distinguishable role
794 of eDNA in the viscoelastic relaxation of biofilms. *MBio* 2013; 4:e00497-13; PMID:
795 24129256; DOI: 10.1128/mBio.00497-13 [doi].
- 796 [39] Bauer S, Kirschning CJ, Hacker H, Redecke V, Hausmann S, Akira S, Wagner H, Lipford
797 GB. Human TLR9 confers responsiveness to bacterial DNA via species-specific CpG motif
798 recognition. *Proc Natl Acad Sci U S A* 2001; 98:9237-42; PMID: 11470918; DOI:
799 10.1073/pnas.161293498 [doi].
- 800 [40] Khalaf H, Lonn J, Bengtsson T. Cytokines and chemokines are differentially expressed in
801 patients with periodontitis: Possible role for TGF-beta1 as a marker for disease progression.
802 *Cytokine* 2014; 67:29-35; PMID: 24680479; DOI: 10.1016/j.cyto.2014.02.007 [doi].
- 803 [41] Lee SY, Choi JH, Xu Z. Microbial cell-surface display. *Trends Biotechnol* 2003; 21:45-52;
804 PMID: 12480350.
- 805 [42] Bauer ME, Townsend CA, Doster RS, Fortney KR, Zwickl BW, Katz BP, Spinola SM,
806 Janowicz DM. A fibrinogen-binding lipoprotein contributes to the virulence of *Haemophilus*

807 ducreyi in humans. *J Infect Dis* 2009; 199:684-92; PMID: 19199547; DOI: 10.1086/596656;
808 10.1086/596656.

809 [43] Fusco WG, Elkins C, Leduc I. Trimeric autotransporter DsrA is a major mediator of
810 fibrinogen binding in *Haemophilus ducreyi*. *Infect Immun* 2013; 81:4443-52; PMID:
811 24042118; DOI: 10.1128/IAI.00743-13 [doi].

812 [44] Kaplanski G, Marin V, Montero-Julian F, Mantovani A, Farnarier C. IL-6: A regulator of
813 the transition from neutrophil to monocyte recruitment during inflammation. *Trends*
814 *Immunol* 2003; 24:25-9; PMID: 12495721; DOI: S1471490602000133 [pii].

815 [45] Scheller J, Chalaris A, Schmidt-Arras D, Rose-John S. The pro- and anti-inflammatory
816 properties of the cytokine interleukin-6. *Biochim Biophys Acta* 2011; 1813:878-88; PMID:
817 21296109; DOI: 10.1016/j.bbamcr.2011.01.034 [doi].

818 [46] Chomarar P, Banchereau J, Davoust J, Palucka AK. IL-6 switches the differentiation of
819 monocytes from dendritic cells to macrophages. *Nat Immunol* 2000; 1:510-4; PMID:
820 11101873; DOI: 10.1038/82763 [doi].

821 [47] McLoughlin RM, Jenkins BJ, Grail D, Williams AS, Fielding CA, Parker CR, Ernst M,
822 Topley N, Jones SA. IL-6 trans-signaling via STAT3 directs T cell infiltration in acute
823 inflammation. *Proc Natl Acad Sci U S A* 2005; 102:9589-94; PMID: 15976028; DOI:
824 0501794102 [pii].

825 [48] Curnow SJ, Scheel-Toellner D, Jenkinson W, Raza K, Durrani OM, Faint JM, Rauz S,
826 Wloka K, Pilling D, Rose-John S, et al. Inhibition of T cell apoptosis in the aqueous humor
827 of patients with uveitis by IL-6/soluble IL-6 receptor trans-signaling. *J Immunol* 2004;
828 173:5290-7; PMID: 15470075; DOI: 173/8/5290 [pii].

829 [49] Cochran DL. Inflammation and bone loss in periodontal disease. *J Periodontol* 2008;
830 79:1569-76; PMID: 18673012; DOI: 10.1902/jop.2008.080233 [doi].

831 [50] Yasuda H, Shima N, Nakagawa N, Yamaguchi K, Kinosaki M, Mochizuki S, Tomoyasu A,
832 Yano K, Goto M, Murakami A, et al. Osteoclast differentiation factor is a ligand for
833 osteoprotegerin/osteoclastogenesis-inhibitory factor and is identical to TRANCE/RANKL.
834 *Proc Natl Acad Sci U S A* 1998; 95:3597-602; PMID: 9520411.

- 835 [51] Tamura T, Udagawa N, Takahashi N, Miyaura C, Tanaka S, Yamada Y, Koishihara Y,
836 Ohsugi Y, Kumaki K, Taga T. Soluble interleukin-6 receptor triggers osteoclast formation
837 by interleukin 6. *Proc Natl Acad Sci U S A* 1993; 90:11924-8; PMID: 8265649.
- 838 [52] Hashizume M, Hayakawa N, Mihara M. IL-6 trans-signalling directly induces RANKL on
839 fibroblast-like synovial cells and is involved in RANKL induction by TNF-alpha and IL-17.
840 *Rheumatology (Oxford)* 2008; 47:1635-40; PMID: 18786965; DOI:
841 10.1093/rheumatology/ken363 [doi].
- 842 [53] Hajishengallis G. Periodontitis: From microbial immune subversion to systemic
843 inflammation. *Nat Rev Immunol* 2015; 15:30-44; PMID: 25534621; DOI: 10.1038/nri3785
844 [doi].
- 845 [54] Lowry OH, Rosebrough NJ, Farr AL, Randall RJ. Protein measurement with the folin
846 phenol reagent. *J Biol Chem* 1951; 193:265-75.
- 847 [55] Nummelin H, El Tahir Y, Ollikka P, Skurnik M, Goldman A. Expression, purification and
848 crystallization of a collagen-binding fragment of yersinia adhesin YadA. *Acta Crystallogr D*
849 *Biol Crystallogr* 2002; 58:1042-4; PMID: 12037311; DOI: S0907444902005231 [pii].
- 850 [56] Yu C, Ruiz T, Lenox C, Mintz KP. Functional mapping of an oligomeric autotransporter
851 adhesin of *Aggregatibacter actinomycetemcomitans*. *J Bacteriol* 2008; 190:3098-109;
852 PMID: 18310342; DOI: 10.1128/JB.01709-07 [doi].
- 853 [57] Oksanen J, Hormia M. An organotypic in vitro model that mimics the dento-epithelial
854 junction. *J Periodontol* 2002; 73:86-93; PMID: 11846204.
- 855 [58] Mäkelä M, Salo T, Larjava H. MMP-9 from TNF alpha-stimulated keratinocytes binds to
856 cell membranes and type I collagen: A cause for extended matrix degradation in
857 inflammation? *Biochem Biophys Res Commun* 1998; 253:325-35; PMID: 9878537; DOI:
858 10.1006/bbrc.1998.9641.
- 859 [59] Green H, Fuchs E, Watt F. Differentiated structural components of the keratinocyte. *Cold*
860 *Spring Harb Symp Quant Biol* 1982; 46 Pt 1:293-301; PMID: 6179694.

- 861 [60] Wang Y, Goodman SD, Redfield RJ, Chen C. Natural transformation and DNA uptake
862 signal sequences in *Actinobacillus actinomycetemcomitans*. *J Bacteriol* 2002; 184:3442-9;
863 PMID: 12057937.
- 864 [61] Cheng YA, Jee J, Hsu G, Huang Y, Chen C, Lin CP. A markerless protocol for genetic
865 analysis of *Aggregatibacter actinomycetemcomitans*. *J Formos Med Assoc* 2014; 113:114-
866 23; PMID: 24530245; DOI: 10.1016/j.jfma.2012.05.005 [doi].
- 867 [62] Fujise O, Wang Y, Chen W, Chen C. Adherence of *Aggregatibacter*
868 *actinomycetemcomitans* via serotype-specific polysaccharide antigens in
869 lipopolysaccharides. *Oral Microbiol Immunol* 2008; 23:226-33; PMID: 18402609; DOI:
870 10.1111/j.1399-302X.2007.00416.x [doi].
- 871 [63] Sternberg N, Sauer B, Hoess R, Abremski K. Bacteriophage P1 cre gene and its regulatory
872 region. evidence for multiple promoters and for regulation by DNA methylation. *J Mol Biol*
873 1986; 187:197-212; PMID: 3486297; DOI: 0022-2836(86)90228-7 [pii].
- 874 [64] Wang Y, Shi W, Chen W, Chen C. Type IV pilus gene homologs pilABCD are required for
875 natural transformation in *Actinobacillus actinomycetemcomitans*. *Gene* 2003; 312:249-55;
876 PMID: 12909361.
- 877 [65] Lippmann JE, Froeliger EH, Fives-Taylor PM. Use of the *Actinobacillus*
878 *actinomycetemcomitans* leukotoxin promoter to drive expression of the green fluorescent
879 protein in an oral pathogen. *Oral Microbiol Immunol* 1999; 14:321-5; PMID: 10551160.
- 880 [66] Sreenivasan PK, Fives-Taylor P. Isolation and characterization of deletion derivatives of
881 pDL282, an *Actinobacillus actinomycetemcomitans*/*Escherichia coli* shuttle plasmid.
882 *Plasmid* 1994; 31:207-14; PMID: 8029328; DOI: S0147-619X(84)71022-5 [pii].
- 883 [67] Mintz KP, Moskovitz J, Wu H, Fives-Taylor PM. Peptide methionine sulfoxide reductase
884 (MsrA) is not a major virulence determinant for the oral pathogen *Actinobacillus*
885 *actinomycetemcomitans*. *Microbiology* 2002; 148:3695-703; PMID: 12427959; DOI:
886 10.1099/00221287-148-11-3695 [doi].
- 887 [68] Hisano K, Fujise O, Miura M, Hamachi T, Matsuzaki E, Nishimura F. The pga gene cluster
888 in *Aggregatibacter actinomycetemcomitans* is necessary for the development of natural

- 889 competence in Ca(2+) -promoted biofilms. *Mol Oral Microbiol* 2014; 29:79-89; PMID:
890 24450419; DOI: 10.1111/omi.12046 [doi].
- 891 [69] Wu J, Xi C. Evaluation of different methods for extracting extracellular DNA from the
892 biofilm matrix. *Appl Environ Microbiol* 2009; 75:5390-5; PMID: 19561191; DOI:
893 10.1128/AEM.00400-09 [doi].
- 894 [70] Rose SJ, Babrak LM, Bermudez LE. *Mycobacterium avium* possesses extracellular DNA
895 that contributes to biofilm formation, structural integrity, and tolerance to antibiotics. *PLoS*
896 *One* 2015; 10:e0128772; PMID: 26010725; DOI: 10.1371/journal.pone.0128772 [doi].
- 897 [71] Tang G, Mintz KP. Glycosylation of the collagen adhesin EmaA of *Aggregatibacter*
898 *actinomycetemcomitans* is dependent upon the lipopolysaccharide biosynthetic pathway. *J*
899 *Bacteriol* 2010; 192:1395-404; PMID: 20061477; DOI: 10.1128/JB.01453-09 [doi].
- 900 [72] Saarela M, Asikainen S, Alaluusua S, Pyhälä L, Lai CH, Jousimies-Somer H. Frequency and
901 stability of mono- or poly-infection by *Actinobacillus actinomycetemcomitans* serotypes a,
902 b, c, d or e. *Oral Microbiol Immunol* 1992; 7:277-9.
- 903 [73] Slot JW, Geuze HJ. A new method of preparing gold probes for multiple-labeling
904 cytochemistry. *Eur J Cell Biol* 1985; 38:87-93; PMID: 4029177.

905

906 Figure Legends

907 **Figure 1.** BilRI is an IDP lacking a specific fold without a binding ligand. A) ^1H spectrum of BilRI
908 (pH 7.0, 25°C) at 600 MHz. The lack of signal dispersion in the ^1H methyl (< 1 ppm) and amide
909 proton ($^1\text{H}^{\text{N}}$, 7-8 ppm) regions is indicative of the disordered nature of BilRI in solution. B) ^1H - ^{15}N
910 correlation spectrum (^{15}N -HSQC) of BilRI (pH 5.0, 25°C) at 800 MHz. A two-dimensional ^1H - ^{15}N
911 correlation map highlights the poorly dispersed $^1\text{H}^{\text{N}}$ region, confirming observations of the intrinsic
912 disorder of BilRI, based on a ^1H spectrum at 600 MHz at pH 7. C) Amino acid sequence analysis
913 confirmed the IDP nature of BilRI. The high proportions of either polar (blue) or charged (magenta)
914 and the low numbers of bulky hydrophobic (yellow) amino acids are typical for IDPs.

915 **Figure 2.** BilRI bound to various human inflammatory cytokines but not to fibrinogen or collagen. A)
916 Recombinant BilRI containing an 8-histidine-long C-terminal tag bound to various recombinant
917 human cytokines in a microplate assay. BSA served as a negative control and was used as a blocking
918 agent in the assays. The bound BilRI was detected with HRP-labelled HisProbeTM. The BilRI binding
919 to IL-8 was high compared to the binding to the control protein BSA (**:p=0.008, paired-samples T-
920 test). B) Recombinant BilRI containing an 8-histidine-long C-terminal tag did not bind to fibrinogen-
921 coated wells in a microplate assay when detected with europium-labelled antibody against the
922 histidine tag. Although the positive control recombinant ClfA of *S. aureus* bound fibrinogen
923 efficiently, the recombinant FgbA, which has been reported to bind fibrinogen,⁴² did not show
924 positive binding in the assay. Only BilRI binding to IL-8 showed a statistically significant positive
925 difference compared with the BSA control (p=0.028, Mann-Whitney U-test) from the test
926 experiments. C) Recombinant BilRI containing an 8-histidine-long C-terminal tag did not bind to
927 collagen-coated wells in the microplate assays when detected with europium-labelled antibody against
928 the histidine tag. The positive control recombinant YadA of *Y. enterocolitica* bound collagen
929 efficiently. Only BilRI binding IL-8 showed a statistically significant positive difference compared
930 with control BSA (p=0.028, Mann-Whitney U-test) from the test experiments.

931 **Figure 3.** Viable wild-type *A. actinomycetemcomitans* biofilm bound IL-8 and IL-6, and internalized
932 IL-1 β when co-cultured with organotypic gingival mucosa. A) *A. actinomycetemcomitans* wild-type

933 biofilm bound both IL-8 and IL-6 when co-cultured with organotypic gingival mucosa in the absence
934 of the antibiotics penicillin and streptomycin. In the presence of these antibiotics, the biofilm bound
935 less IL-8 and IL-6 whereas the epithelium contained elevated amounts of IL-8 and IL-6. B) The
936 amount of IL-8 produced was approximately ten times the amount of IL-6 in the organotypic gingival
937 mucosa tissue culture model. The co-culture system released slightly more IL-8 and IL-6 to the
938 culture medium when stimulated with *A. actinomycetemcomitans* biofilm in the presence of
939 antibiotics than in the absence of antibiotics. Due to the standard deviation between the samples, the
940 difference was not statistically significant. N=3. C) In the organotypic gingival tissue culture model,
941 which produced approximately 200 pg of IL-1 β to the culture medium during a 24-h incubation with
942 viable *A. actinomycetemcomitans* wild-type biofilm,²⁸ the uptake efficiency of IL-1 β was estimated by
943 counting the number of gold particles in anti-IL-1 β -stained immuno-EM samples.

944 **Figure 4.** The outer membrane lipoprotein BilRI was not essential for the formation of typical *A.*
945 *actinomycetemcomitans* rough-type colonies, biofilm or cell size and shape. BilRI overexpression-
946 induced lysis of the outer membrane resulted in tiny colonies and significantly reduced biofilm
947 amounts. A) On blood agar plates, the *bilRI* mutant formed typical rough-type colonies, whereas the
948 BilRI-overexpressing strain (*bilRI* rev) formed very tiny colonies (circled in white). B) Uniform cell
949 suspensions could be produced similarly with the wild-type and *bilRI* mutant strains following the
950 method described by Karched et al.³¹ Because the BilRI-overexpressing strain *bilRI* rev grew slowly
951 on agar plates, it was difficult to harvest a sufficient cell mass to obtain a dense cell suspension. C)
952 The *bilRI* mutant formed as much biofilm as the wild-type strain after 20-24 hours, as estimated
953 through Crystal violet staining.³² The overexpression of BilRI almost completely eliminated the
954 capacity of the strain (*bilRI* rev) to form biofilm (***:p=0.0003, paired-samples T-test with
955 Bonferroni corrections). D) Transmission electron microscopy revealed that the shape and size of the
956 *bilRI* mutant cells resembled those of wild-type cells. The overexpression of BilRI (*bilRI* rev) lysed
957 the bacterial outer membrane, resulting in a smaller cell size. Arrows indicate the *A.*
958 *actinomycetemcomitans* cells in images in which other structures, such as the filter disc, are visible.

959 **Figure 5.** *A. actinomycetemcomitans bilRI* mutant cells differed from wild-type cells in the
960 composition of the biofilm and their capacity to bind collagen and fibrinogen. A) The *bilRI* mutant
961 biofilm contained more total protein than the corresponding *A. actinomycetemcomitans* wild-type
962 strain. N=7, ** p=0.009 (Mann-Whitney U-test). B) The *bilRI* mutant biofilm contained less eDNA
963 than the corresponding *A. actinomycetemcomitans* wild-type strain. N=4, * p=0.021 (Mann-Whitney
964 U-test). C) *A. actinomycetemcomitans bilRI* mutant cells did not differ significantly from the wild-
965 type cells in terms of binding to collagen-coated or fibrinogen-coated wells.

966 **Figure 6.** *A. actinomycetemcomitans* wild-type and *bilRI* mutant strains internalized all tested
967 inflammatory cytokines: IL-1 β , IL-8 and IL-6. The outer membrane lipoprotein BilRI had a role in the
968 uptake of only IL-1 β in the test system. A) Both *A. actinomycetemcomitans* wild-type and *bilRI*
969 mutant biofilm cells internalized IL-1 β , IL-8 and IL-6 when incubated for 24 h with human gingival
970 keratinocyte monolayers. Cytokine uptake was studied with anti-cytokine IgG antibodies combined
971 with protein A-gold labelling and transmission electron microscopy. B) Deletion of the *bilRI* gene
972 decreased only IL-1 β uptake (p=0.007, Mann-Whitney U-test), while IL-8 and IL-6 uptake levels
973 were not affected. The uptake efficiencies were estimated by counting the amounts of gold labelling
974 in the positively stained cells.

975 **Figure 7.** The produced recombinant proteins YadA (23 kDa), ClfA (36 kDa), FgbA (12 kDa), IL-8
976 (9 kDa) and BilRI (18 kDa) were pure, as observed in a Coomassie-stained SDS-PAGE gel. A total
977 amount of 1 μ g of each protein was run in the gel.

978 Tables

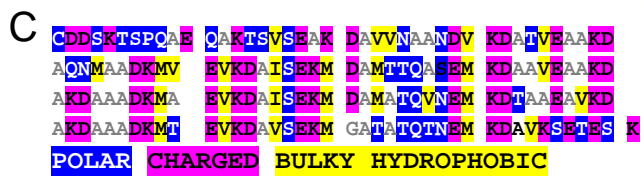
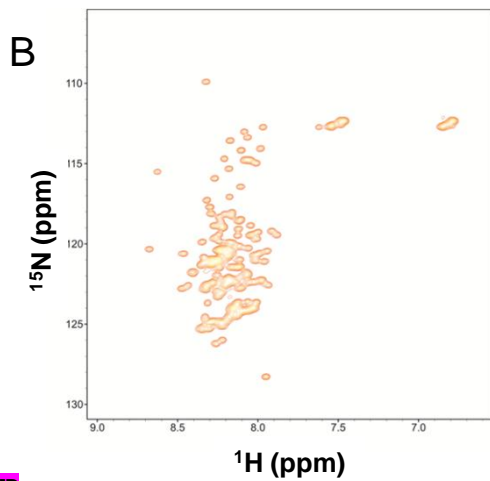
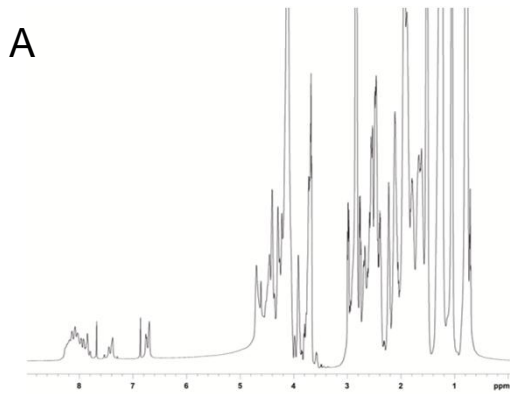
979 **Table 1.** The nucleotide sequences of primers that were used in producing the markerless *bilRI*
 980 deletion mutant of *A. actinomycetemcomitans* D7S.

Primer name	Sequence
bilRI_nest-F	5`- GTATGGTGCCTGACTTTCCGG-3
bilRI_nest-R	5`-TTATGGTGGATCACCTTGGT-3`
ycgL-FD	5`CCAAGGCTGGAAAGCGATATT-3`
bilRI_RD_BamHI	5'-CTAGGATCCTGAAAGCAAATAAAAAAGCAGTCTA-3'
phoGlu-R	5`-GCGACCAAGCCTTATTTA -3`
sixA_FD_SalI	5'- CGT <u>GTC GAC</u> TTA ATA TAG GTC AAA ATT TAT CT -3'

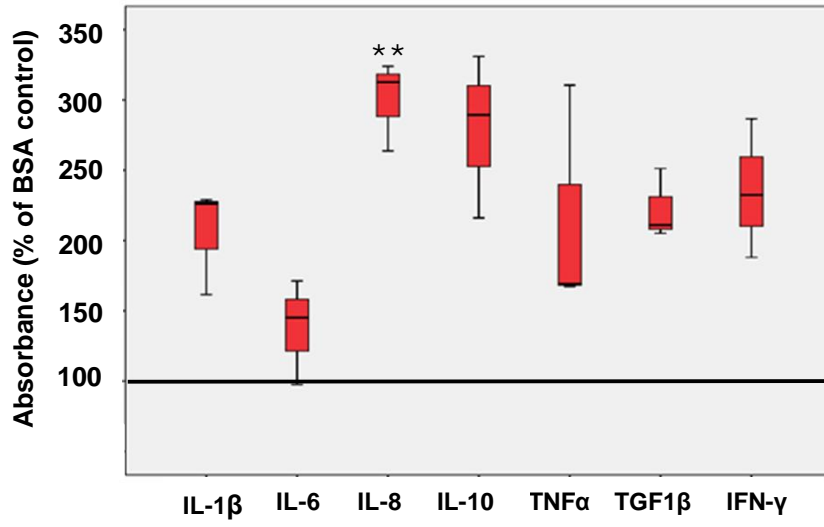
981 **Table 2.** Effect of the cytokines IL-1 β and IL-8 (22 h incubation) on the amount and composition of
 982 pre-formed *A. actinomycetemcomitans* D7S wild-type (wt) and *bilRI* mutant biofilms. The data are
 983 shown as the means \pm SD from four independent experiments. The statistically significant differences
 984 ($p \leq 0.05$, Mann-Whitney U-test with Bonferroni corrections) between the cytokine-treated and
 985 cytokine-untreated biofilms are given in parenthesis.

Strain	Cytokine	Percentage of the control (without cytokines)			
		Biofilm mass	eDNA	PGA	Total protein
D7S wt	IL-1 β	94 \pm 7	56 \pm 16 (0.018)	89 \pm 8	86 \pm 17
D7S wt	IL-8	96 \pm 12	63 \pm 23 (0.028)	88 \pm 15	88 \pm 19
D7S <i>bilRI</i>	IL-1 β	92 \pm 5	106 \pm 26	94 \pm 7	89 \pm 9
D7S <i>bilRI</i>	IL-8	104 \pm 11	103 \pm 22	89 \pm 9	94 \pm 32

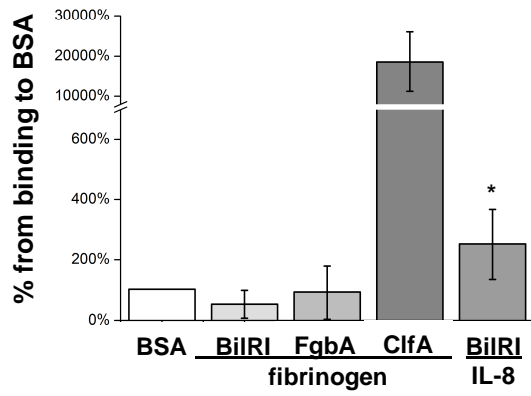
986



A



B



C

